Effect of Organoclay in an Immiscible Poly(ethylene terephtalate) Waste/Poly(methyl methacrylate) Blend

N. Kerboua,[1,2] N. Cinausero,[2] T. Sadoun,[1] J. M. Lopez-Cuesta[2]

[1]*Laboratoire des Matériaux Organiques, Université A.MIRA de, Béjaia 06000, Algeria*
[2]*Ecole des Mines d'Alès, Centre des Matériaux de Grande Diffusion (CMGD), 6 Av. de Clavières, Alès 30319, France*

Received 20 May 2009; accepted 2 November 2009
DOI 10.1002/app.31968
Published online 2 March 2010 in Wiley InterScience (www.interscience.wiley.com).

ABSTRACT: Blends of organically modified montmorillonite (OMMT) with poly(ethylene terephtalate) (PET) waste and poly(methyl methacrylate) (PMMA) were prepared by melt mixing. The morphology of PET/PMMA nanocomposites with different OMMT contents was characterized by transmission electron microscopy (TEM) and X-ray diffraction (XRD). The nonisothermal crystallization temperatures of nanocomposites were also examined by DSC. TEM observations and XRD patterns revealed that silicate layers were intercalated and well dispersed in the blend. Nanocomposites displayed better mechanical properties when compared with the unfilled blend. DMA analyses also showed efficient mixing of the two immiscible polymers and changes in glass transition temperature with the presence of OMMT. DSC analysis showed an enhancement in crystallization rate of nanocomposites and a decrease in cristallinity. © 2010 Wiley Periodicals, Inc. J Appl Polym Sci 117: 129–137, 2010

Key words: compatibilization; blend; montmorillonite; poly(ethylene terephtalate); poly(methyl methacrylate); nonisothermal crystallization temperature

INTRODUCTION

The commercial development of polymer blends has become important because production of blends are more favorable economically compared to the more conventional chemical routes for making new products. In the area of polymer blends and alloys, the word compatibilizer refers usually to a macromolecule used to modify the interfacial properties of two immiscible polymers. Such a macromolecule may be a homopolymer or a block, graft, or star copolymer generated in or *ex* situ.[1–4] Its presence could refine the droplet size of the dispersed minor phase is stabilizing it against coalescence during melt mixing and ensuring strong interfacial adhesion between the phases in the solid state, thus improving the final mechanical properties. This kind of classical compatibilization strategy has been widely used to produce a variety of industrial polymer blends with a wide range of controlled properties.[5,6] Moreover, in some cases, the presence of inorganic solid particle can play a role of compatiblizer and in order to achieve this function, the specific surface area of inorganic particles should be as large as possible. This requirement is satisfied with layered silicates such as clays.[7–9]

Nowadays millions of tons of poly(ethylene terephtalate) PET scrap are produced annually all over the world. This scrap mostly comes from beverage bottles of short life cycle. Their reuse can lead to the manufacture of new products by reprocessing. However, PET recycling is a complex process because of chemical and mechanical degradation during reprocessing caused by the temperature, and the presence of moisture and contaminations.[10–12] These properties can be improved by blending this polymer with another one presenting good properties. In the literature, there have been numerous articles on various aspects of binary blends of polyesters, including blends of PET, poly(butylene terephtalate) (PBT),[13,14] poly(trimethylene terephtalate) (PTT), polycarbonate (PC),[15,16] and polyetherimide (PEI).[17] The reactive compatibilization of model blends of PET and polyolefins has been also examined in several articles.[18,19] In this work, we have chosen to blend PET with PMMA. The first reason for choosing this polymer pair was that PMMA is a rigid commodity thermoplastic material, which can be found in waste plastics mixtures, as minor component, while PET is a ductile engineering polymer. Hence, it seems interesting to blend these two polymers to get a material with original properties. Commercial Blends, of PMMA and PET are commercially available from Rohm and Hass under the trade name Ropet.[20] These blends are fiberglass reinforced and designed

Correspondence to: J. M. Lopez-Cuesta (Jose-Marie.Lopez-Cuesta@ema.fr).

for automotive and electrical markets. They offer low warpage and fast molding cycle. Nevertheless, other kind of reinforcements can be proposed for such blends and the objective of this work was to study the phase structure and properties of an immiscible PET/PMMA blend, in the presence of organically modified montmorillonite (OMMT) and to assess modifications of blend morphologies. Besides, only a few studies on polymer blends based nanocomposites.[7,8] and more precisely on PET/PMMA blends[4,21–24] have been investigated. Furthermore, no article has dealt with PET waste/PMMA blend.

The effect of organically modified montmorillonite content on phase morphology, thermal behavior, and mechanical properties were investigated by scanning electron microscopy (SEM), dynamic mechanical analysis (DMA), and mechanical testing in traction mode. The dispersion of silicate layers in the clay containing blend was also characterized by X-ray diffraction (XRD) and transmission electron microscopy (TEM). To assess the effect of blend composition on degree of crystallinity and the rate crystallization DSC analysis was used.

EXPERIMENTAL

Materials

Postconsumer bottle flakes of recycled PET (PETP218/4003) were supplied by SOREPLA INDUSTRIE, a PET recycling company ($\eta_{PET} = 0.76$ dl/g, in 2-chlorophenol at 25°C).The fraction of contaminants was less than 50 ppm. PMMA used was a commercial Altuglas V825T (M_w = 93,000 g/mol) from Arkema Group.

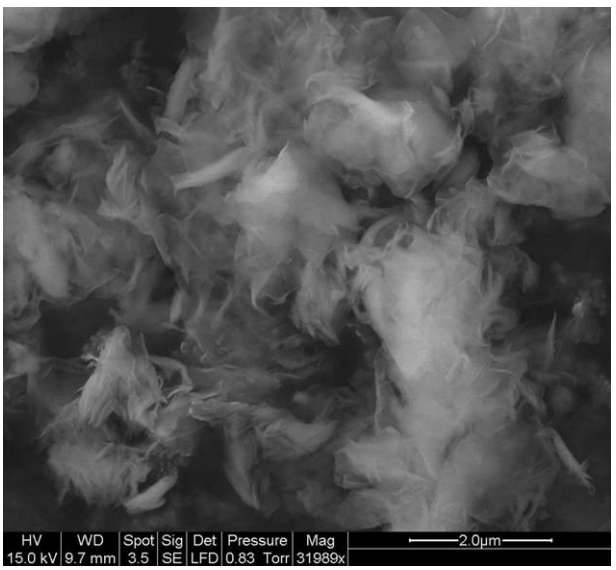

Figure 1 SEM micrograph of Nanofil2 (X 31,989).

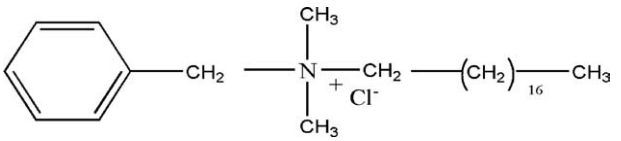

Scheme 1 Organophilization agent of Nanofil 2.

The organically modified montmorillonite (OMMT) used in this study was Nanofil 2 from Rockwood (modified with quaternary ammonium salt: benzyl (hydrogenated tallow alkyl)dimethyl). A micrograph of Nanofil 2 is shown in Figure 1. The chemical structure of the organophilization agent as presented in Scheme 1.

Polymer processing

Before melt mixing, the two homopolymers and the organoclay were dried in a vacuum oven, respectively, at 100°C and 60°C overnight. Blending was performed in a twin-screw co-rotating extruder CLEXTRAL BC 21 (L = 1200 mm, L/D = 48) with screw configuration designed to promote Nanofil 2 dispersion. The modified montmorillonite was introduced in the melted zone of the extruder. The selected compositions are given in Table I.

Extrusion conditions were the same for all compositions: feed rate (Q) = 4 kg/h and screw speed (N) = 350 rpm. The residence time in the extruder under the above conditions was about 75 s.

Before injection, the pellets were dried under vacuum (100°C, overnight). Injection molding was carried out at 250–265°C using a KRAUSS MAFFEI KM50-180CX machine with a mold temperature of 40°C. The specimens produced were dogbones according to ISO 527-2 type 1A specifications and used for mechanical testing.

Characterization

The blend morphologies were examined by SEM using a QUANTA 200 F apparatus operating at an accelerating voltage of 15 kV. The samples were cryofractured in liquid nitrogen. All the samples were coated with thin layer of carbon prior to SEM observations.

TABLE I
Table of Compositions

Compositions	PET (wt %)	PMMA (wt %)	Nanofil (wt %)
90PET/10PMMA	90	10	0
90PET/10PMMA/1Nanofil2	89.1	9.9	1
90PET/10PMMA/2Nanofil2	88.8	9.8	2
90PET/10PMMA/5Nanofil2	85.5	9.5	5

The XRD patterns were recorded on a BRUKER AXS 08 ADVANCE diffractometer. The beam was Cu Kα radiation (λ = 0.15405 nm) operated at 40 kV and 40 mA. Data were obtained from 2θ = 0° to 60°.

The dispersion of intercalated silicate layers within the blend matrix was examined by TEM using JEOL- 1200EX2 apparatus operating at an accelerating voltage of 120 kV. The TEM specimens were about 70 nm thick. They were prepared by ultramicrotoming (Leica-UCT).

Dynamic mechanical analysis (DMA) of the injection molded rectangular specimens with dimensions of 40 mm × 10 mm x 4 mm were conducted using METRAVIB dynamic analyser at a fixed frequency of 5 Hz and an oscillation amplitude of 1 μm. The temperature studied ranged from 25 to 200°C and the temperature rate was 3°C/min.

Rheological tests were carried out using an ARES Rheometrics Scientific apparatus, equipped with two parallel plates (diameter = 25 mm). All the tests with the ARES were carried out at 260°C with a gap between the plates of 1 mm.

Thermogravimetric analysis (TGA) was conducted on a PerkinElmer Thermogravimetric Analyser at a heating rate of 10°C/min under air, from room temperature to 700°C.

Test specimens for tensile measurements were prepared from 4 mm thick according to ISO 527-2-1A. The tensile modulus and tensile strength were measured in a ZWICK TH010 (load 10 kN) at strain rates of 1 mm/min and 50mm/min, respectively.

A Pyris Diamond DSC- PerkinElmer differential scanning calorimeter was used to record the nonisothermal melt crystallization endotherms of neat PET, PET/PMMA blend and its nanocomposites. All samples were analyzed according the following temperature program in function of time indicated (Fig. 2), with temperature ramps of 5, 10, 20°C/min, for the investigation of crystallization processes of the samples.

The crystalline fraction (X_c) was calculated by integration of the melting and crystallization peaks referring it to theoretical data of melting enthalpy of fully crystalline PET (ΔH 100%c = 135.8 J/g),[25] according to equations:

$$Xc(wt\%) = \frac{\Delta H'}{\Delta H 100\%c} \quad (1)$$

and

$$\Delta H' = \frac{\Delta H \exp}{1 - x} \quad (2)$$

Here, ΔH exp is the difference between the melting enthalpy and crystallization enthalpy measured and x is the organoclay weight fraction.

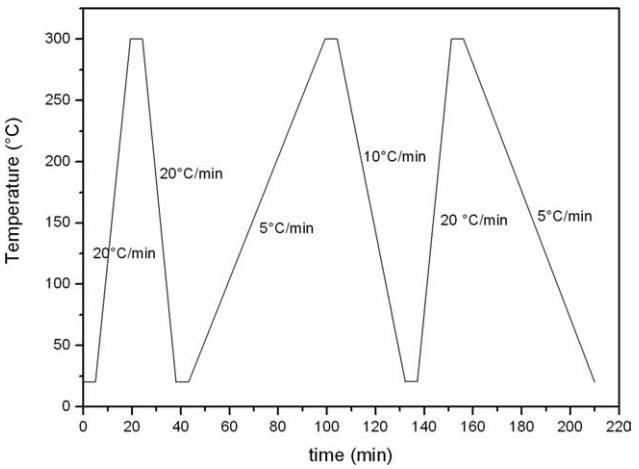

Figure 2 Temperature program for Differential Scanning Calorimetry tests.

The rate of crystallization was calculated according to the formula[26]:

$$CRC = \frac{\Delta \Phi}{\Delta T_c} \quad (3)$$

where Φ is the cooling rate (°C/h) and T_c is the crystallization temperature (°C).

RESULTS AND DISCUSSION

The phase morphologies of both the virgin and filled blends are shown in Figure 3. SEM image of virgin blend clearly demonstrates a two phase structure, indicating the expected immiscibility of the components. SEM image of fracture surface of PET/PMMA with 2 wt % of Nanofil 2 shows that the morphology of the virgin blend was significantly changed and that particles size was dramatically reduced. An increase in Nanofil 2 loading from 2 to 5 wt % leads to a more pronounced decrease in particle size and it becomes impossible to distinguish the dispersed PMMA domains at this magnification. This observation indicates strong interfacial activity with Nanofil 2 for this polymer pair.

Two possible effects may be evoked regarding the dramatic reduction in the dispersed particle size: (i) the increase in the blend viscosity upon the addition of OMMT and (ii) dispersion of intercalated silicate layers in both phases due to common intercalation at the interphase between the two polymers. The viscosity of the virgin and clay-modified blends was also measured. The results are shown in Figure 4(a). This figure shows the change of dynamic viscosity of 90PET/10PMMA virgin blend and 90PET/10PMMA modified blend with 1 to 5 wt % of Nanofil 2 addition. OMMT addition induces a strong

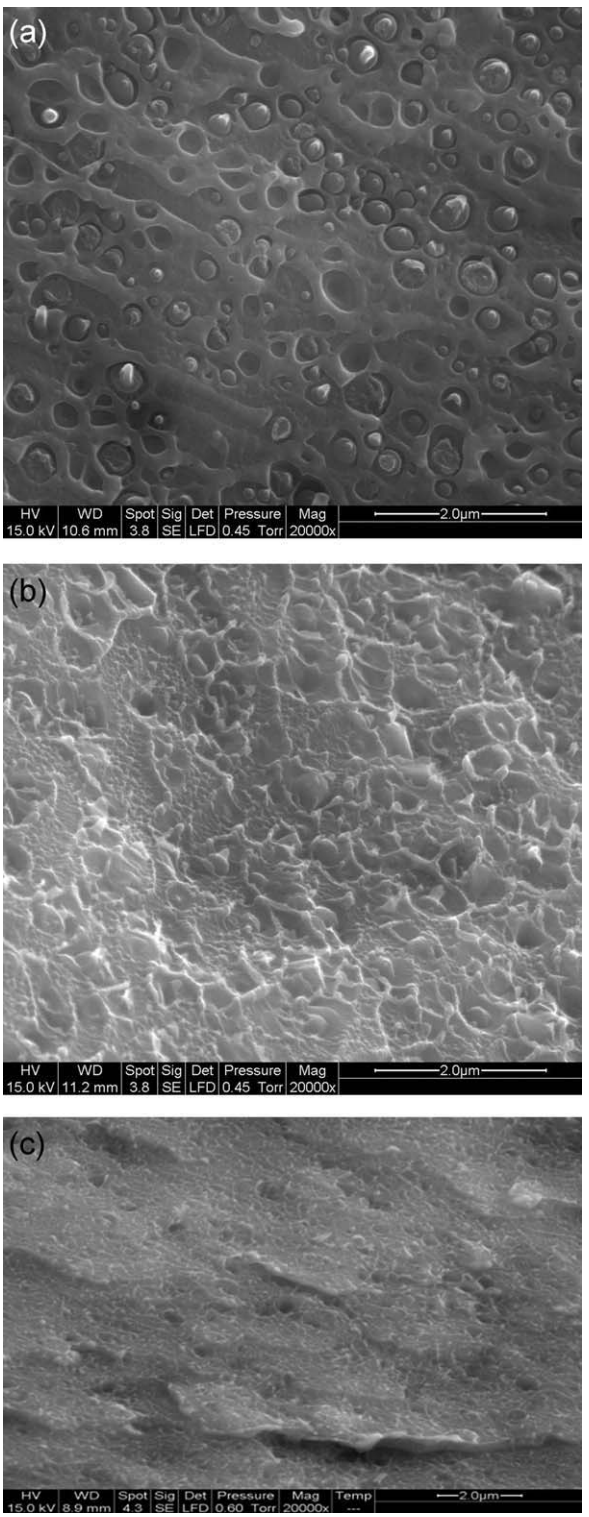

Figure 3 SEM images of the fracture surfaces of virgin 90PET/10PMMA blend and its nanocomposites with Nanofil 2. (a) PET/PMMA (90/10), (b) PET/PMMA/Nanofil (90/10/2), (c) PET/PMMA/Nanofil (90/10/5).

increase in the blend viscosity [Fig. 4(a)] and dynamic storage [Fig. 4(b)] at low frequencies because of dispersion of intercalated silicate layers within the blend matrix. However, only a slight increase in viscosity in

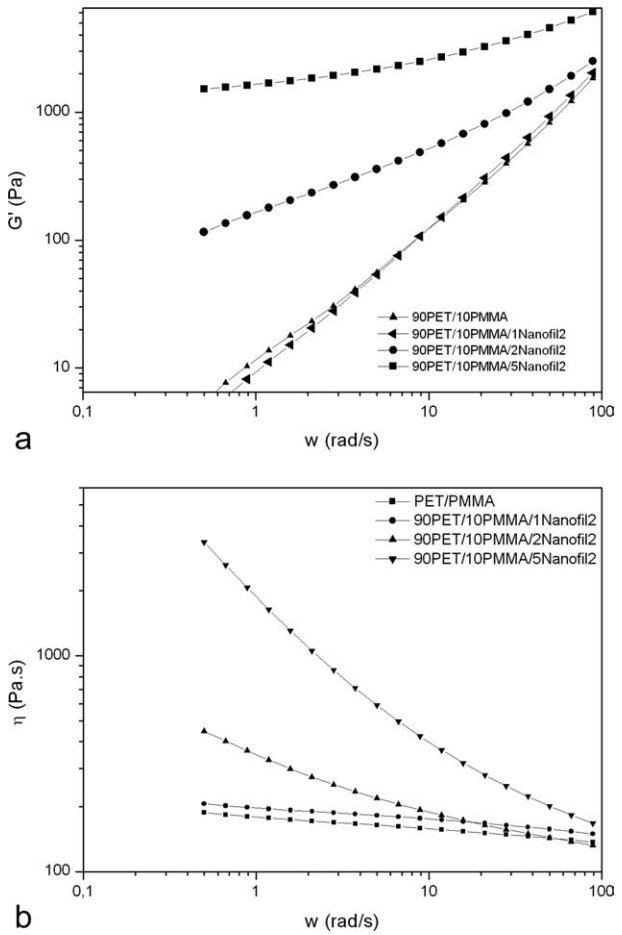

Figure 4 Dynamic viscosity of PET/PMMA neat blend and its nanocomposites as a function of frequency (a), variation of G′ of PET/PMMA blend and its nanocomposites (b).

the high frequency region can be noticed for the most part of filled compositions.

To understand the state dispersion of the silicate layers, XRD analyses were carried out on the pure

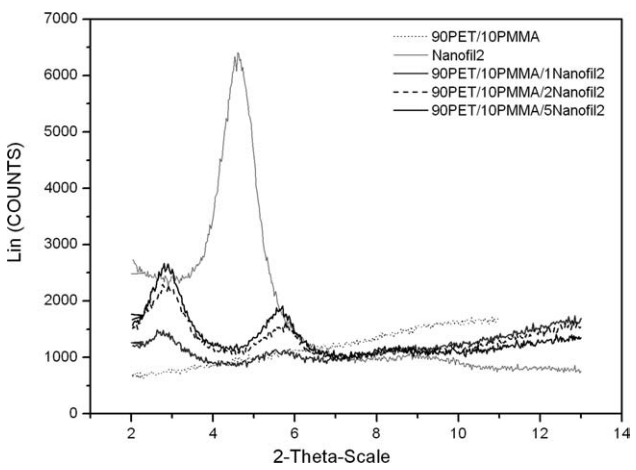

Figure 5 XRD patterns of pure Nanofil2 powder, neat blend and its nanocomposites.

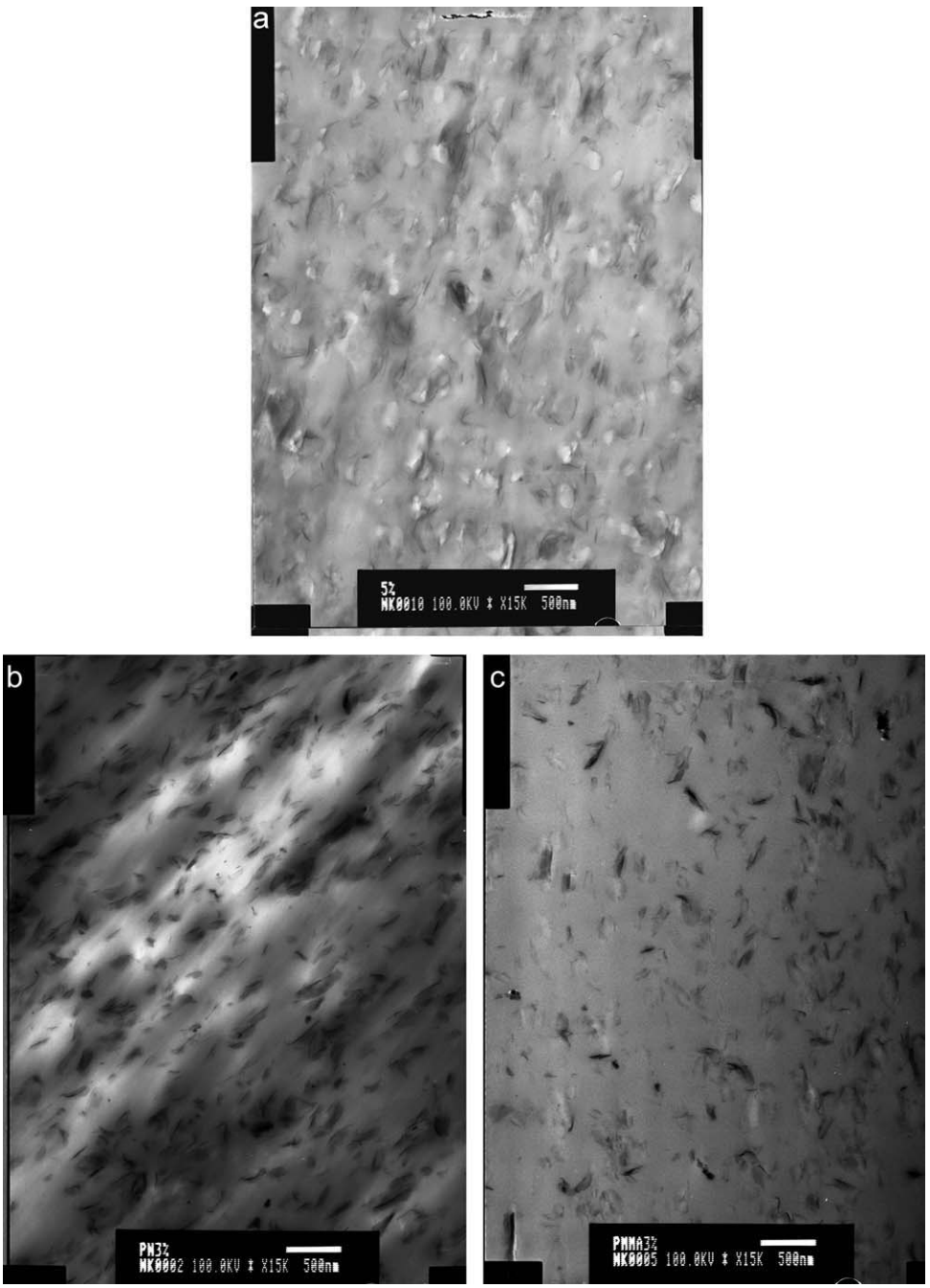

Figure 6 Bright field TEM image of PET/PMMA/Nanofil2 (90/10/5) (a), PET/Nanofil2 (b), PMMA/Nanofil2 (c).

Nanofil 2 powder, PET, PMMA, unfilled 90PET/10PMMA blend, and clay-modified blend.

Figure 5 shows the XRD patterns of pure Nanofil 2 and PET/PMMA blends modified with 1, 2, and 5 wt % addition of Nanofil 2. The characteristic peak (d_{001}) of Nanofil2 was observed at $2\theta = 4.6^\circ$ ($d = 1.97$ nm). The intensity of the characteristic peak of Nanofil 2 in PET/PMMA/1Nanofil2 was reduced and a sharp peak was observed at $2\theta = 2.8^\circ$ ($d = 3.15$), indicating intercalated structure. By increasing the loading of OMMT in 90PET/10PMMA blend from 1 to 2 and 5 wt %, the characteristic peak of Nanofil 2 is slightly shifted toward the higher angles $2\theta = 2.92^\circ$ and 2.95° respectively and at the same time the intensity is decreased. Moreover, the presence of other peaks at higher angles (5.7–5.8°) than in Nanofil 2 seems to show a parallel stacking of the silicate layers. It can be concluded that with 2 or 5 wt % Nanofil 2 in PET/PMMA blend, silicate layers are intercalated and stacked.

To gain more insight into the compatibilization activity of Nanofil2 and its interactions with PET and PMMA homopolymers, TEM analysis was carried out to localize the intercalated silicate layers in the

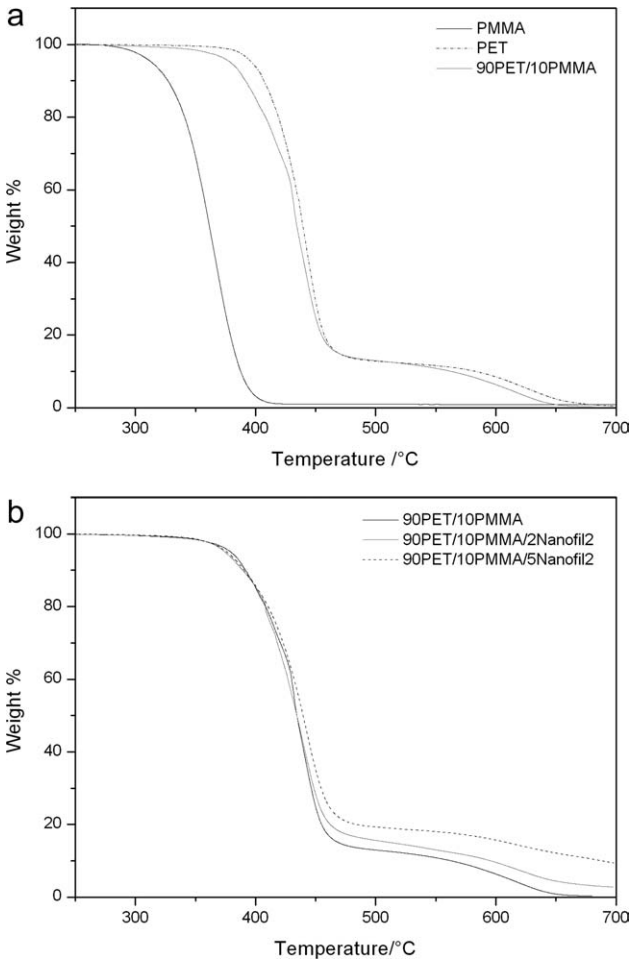

Figure 7 TGA curves for PET waste, virgin PMMA, and PET/PMMA blend (a), TGA curves of PET/PMMA (90/10) blend, PET/PMMA/Nanofil2 (90/10/2 and 90/10/5) (b).

two polymers and the blend (Fig. 6). Figure 6(a) represents TEM images of a 90PET/10PMMA/5Nanofil2. The micrographs reveal that the stacked and intercalated silicate layers (dark entities) are well dispersed within the blend matrix. A possible explanation for this observation is that both PET and PMMA have comparable interactions with Nanofil2 and both are intercalated into the Nanofil 2 silicate layers [Fig. 6(b,c)]. The TEM results are well matched with XRD patterns as reported in Figure 5 as organo-modified clays appears well dispersed in either PMMA, PET alone, or in PET/PMMA blend.

TABLE II
Percentage of Residue, Temperatures for 1 wt % Loss and DTG Peak of PET/PMMA Blend and its Nanocomposites at 700°C

Sample	Residue (%)	1% weight loss (°C)	Tpeak (°C)
PET/PMMA	0	334	440
PET/PMMA/1% Nanofil2	1.4	336	441
PET/PMMA/2% Nanofil2	2.8	340	443
PET/PMMA/5% Nanofil2	9.4	343	446

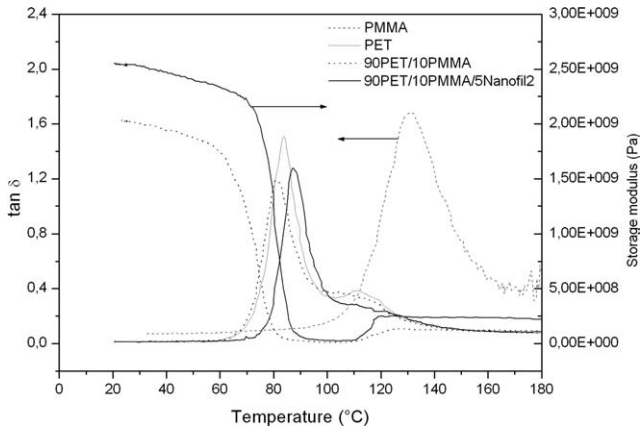

Figure 8 Storage modulus and tan δ vs temperature for PET/PMMA blend and its nanocomposite.

The thermal degradation features of Nanofil 2 were investigated using TGA under air at dynamic (ramp of 10°C/min) and isothermal conditions (260°C). Taking into account the short residence time during processing, it is clear that Nanofil 2 would only loss 5 wt % at the maximum, because of the degradation of the organic modifier.

The thermal stability of the samples was also studied by TGA. Although PMMA has much weaker thermal stability than virgin PET, the stability of the blend with 90 wt % of PET is almost not affected from 450°C [Fig. 7(a)]. Some interactions between PET and PMMA might occur to stabilize the blend residues all at high temperatures. When Nanofil 2 is incorporated, the thermal degradation is slowed down from 440°C [Fig. 7(b)]. The presence of stacked and intercalated silicate layers may be the main reason for the enhanced thermal stability of the nanocomposites. Organo-modified clay can possibly migrate towards the sample surface and act as a heat barrier enhancing the overall thermal stability of the blend, as well as char promoter after thermal decomposition.[27] From TGA data, 90PET/10PMMA blend

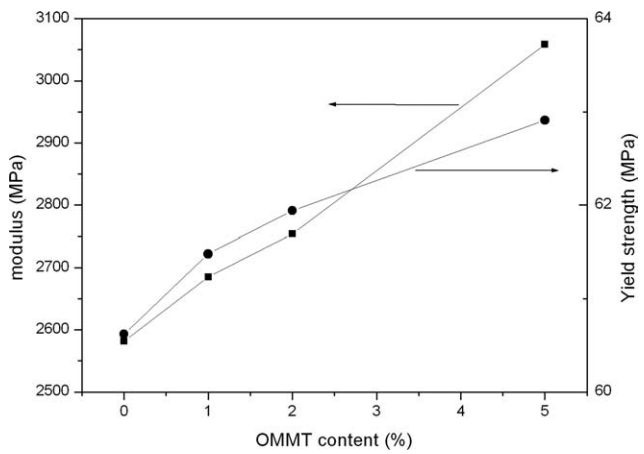

Figure 9 Tensile test results of neat blend (90PET/10PMMA) and its nanocomposites.

TABLE III
Effect of Cooling Rate on Nonisothermal Crystallization of PET/PMMA Alloys

Cooling rate (°C/min)	Onset of cristallization (°C)				Cristallization peak (°C)			
	100/0	95/5	90/10	80/20	100/0	95/5	90/10	80/20
5	223.87	224.3	228.34	228.64	213.85	213.36	217.98	216.85
10	220.16	220.18	226.69	224.94	209.88	208.79	213.33	211.24
20	218	216.47	222.56	220.42	205.33	203.35	206.64	205.75

onset temperature of degradation is 334°C (T_{onset}, weight loss of 1%), while T_{onset} of 90PET/10PMMA/2Nanofil2 and 90PET/10PMMA/5Nanofil2 are 340 and 343°C respectively (Table II). T_{onset} and T_{peak} increases by adding OMMT, as shown by Wang et al.[28] The improvement of the thermal stability of the nanocomposites is likely to be due to an ablative reassembling of the layers sheets, which may occur on the surface of the nanocomposites creating a physical protective barrier on the surface of the material. Besides, according to Liu et al.[29] Volatilization might also be delayed by the labyrinth effect of the silicate layers dispersed in the nanocomposites.

Dynamic mechanical analysis was used to examine the effect of clay addition on glass transition temperature (T_g), of 90PET/10PMMA blend (Fig. 8). PET has much lower T_g (83°C) than PMMA (131°C). The DMA curve of 90PET/10PMMA blend shows two distinct T_g, revealing phase separation in agreement with the SEM results.

The DMA curve for 90PET/10PMMA/5Nanofil2 showed only one sharp T_g at 87.3°C. A unique T_g is generally taken as evidence of constituent miscibility. In addition, the convergence to a single T_g is not symmetrical in the case of the 90PET/10PMMA/5Nanofil2 blend.

The glass transition of miscible blend is usually described by either the Fox law:

$$1/T_g = w_1/T_{g_1} + w_2/T_{g_2}$$

Or by the additive law:

$$T_g = w_1.T_{g_1} + w_2.T_{g_2},$$

where w_1, w_2, T_{g_1} and T_{g_2} are the weight fractions and glass transition temperature of the blend constituents, respectively. The calculated T_g, which are 87.5°C from the Fox law and 87.8°C from the additive law, which are close to that found by DMA analysis. So we can conclude that the clay may induce additional ester–ester exchange reactions between PET and PMMA at 260°C, which can further improve compatibility of the blend.

The dynamic mechanical analysis was also used to investigate the viscoelastic properties of the blend and its nanocomposite as a function of temperature. The storage modulus is also shown in Figure 8 for the neat blend and the 5 wt % clay filled blend. The modulus increases with the addition of clay. Thus, the dispersion of the clay at the nanoscale in the polymer matrix affects the resulting thermo mechanical properties of the nanocomposite.[28]

To confirm the compatibilization effect of Nanofil 2 for the immiscible 90PET/10PMMA blend, the mechanical properties of neat and Nanofil 2-modified blends were studied in traction mode. The results are reported in Figure 9. An enhancement of strength and modulus when adding Nanofil 2 was noticed and ascribed to the good dispersion of organically modified montmorillonite within the polymer matrix. Moreover, the tensile modulus and strength of the nanocomposites blend systematically increased with increasing the loading of Nanofil 2. This is consistent with the previous micrographs (Fig. 3), which shows a high level of mixing due to the strong interactions between the polymers and

Nanofil 2 induced by the large surface area of nanofillers.[28] Consequently, Nanofil 2 acts not only as interfacial active agent that promotes adhesion between the immiscible phases, but also as reinforcing nanofiller.

Nonisothermal crystallization of PET/PMMA blend and its nanocomposites was studied by DSC. Pristine PET is a well know semi-crystallization polymer with a character of low rate of crystallization. The enhancement of its crystallization rate is frequently required in industrial processes involving injection molding procedures. The alloying of PET

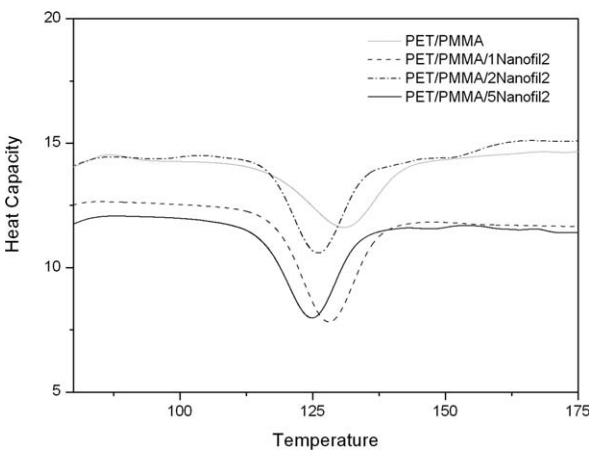

Figure 10 DSC of PET/PMMA/OMMT curves of first heating (rate 20°C/min).

TABLE IV
DSC Crystallization features of PET/PMMA Blends and Nanocomposites (T_{CC} and T_m Are Respectively the Cold Crystallization and Melting temperatures, ΔH_{cc}, ΔH_m, X_c and CRC Are Respectively the Cold Crystallization and Melting enthalpies, the Crystalline Fraction and Crystallization rate)

Sample	Tcc (°C)	Hcc (KJ/Kg)	Tm (°C)	Hm (KJ/Kg)	Xc (%)	CRC (h^{-1})
PET	137	−26.08	255	62.45	27	91.5
PET/PMMA	131.04	−16.45	252.83	45.83	21.64	92.59
PET/PMMA 1%Nanofil2	128.03	−15.33	252	42.50	20.2	94.45
PET/PMMA 2%Nanofil	126.02	−17.89	253.21	40.56	17.03	95.33
PET/PMMA 5%Nanofil	126.73	−22.95	253.87	37.30	12.4	96.5

with PMMA has been found to accelerate the crystallization of PET. At temperatures exceeding 200°C, PET crystallizes in the presence of melted PMMA, while at low temperature, it crystallizes in the presence of solidified PMMA.[21] Table III summarizes the onset temperature and temperature of crystallization of PET and its blends with PMMA at different cooling rates. It is clear from Table III that the crystallization of PET in the alloys is composition dependent and that the 90PET/10PMMA blend crystallizes at a higher temperature indicating enhanced nucleation due to the presence of PMMA.

The crystallization temperature and crystalline content of 90PET/10PMMA blend and its nanocomposites are shown in Figure 10 and Table IV. It can be noticed that the crystallization temperatures decreases upon clay addition. This indicates that Nanofil 2 promotes nucleation of the crystalline PET, and a small amount of organoclay is enough to maximize the nucleation effect. It is interesting to note that the enthalpy of melting is significantly higher than the enthalpy of recrystallization. The crystalline content decreased from 21.64% in 90PET/10PMMA to around 12% with 5% Nanofil 2. This confirms the compatibilization effect of Nanofil 2 in the immiscible 90PET/10PMMA blend since PET crystallization is inhibited. In addition, the crystallization rate at different cooling rate (Table IV) is increased with clay addition. This can be ascribed to the role of effective heterogeneous nucleating agent played by Nanofil 2. OMMT nanostructure itself can help the PET molecules stack located on its vicinity to grow into crystallites.

CONCLUSION

The objective of this work was to investigate the properties of recycled PET/PMMA blends, in which recycled PET is the main component. The incorporation of an organo-modified montmorillonite was also studied to improve the compatibility of such blends and to enhance the mechanical, processing properties as well as the thermal stability.

Various characterizations were used to study the interfacial activity of Nanofil 2 in an immiscible PET/PMMA blend prepared by melt blending including SEM, XRD, TEM, DMA, TGA and finally static mechanical tests in traction mode. By adding the organoclay to 90PET/10PMMA blend, the domain size of the dispersed PMMA decreased considerably. The organoclay content was found to have an important effect on the morphology of PET/PMMA blend. As 2–5 wt % clay additions can induce dramatic decrease in PMMA particles size. XRD diffraction patterns have revealed stacked and intercalated structure for the Nanofil 2 modified blends. TEM observations were found in accordance with the XRD patterns. The glass transition temperature of neat blend was changed in the presence of Nanofil 2 due to morphologic changes and possibly catalytic activity on transesterification processes in the presence of layered silicate particles. Tensile modulus and strength of virgin blend were improved with incorporation of organo-modified clay. The effect of Nanofil 2 on non isothermal crystallization kinetics and cristallinity fraction of 90PET/10PMMA blend were studied using differential scanning calorimetry and it was found that addition of organoclay in 90PET/10PMMA could enhance the rate of crystallization, decrease T_{cc} and cristallinity fraction.

References

1. Schwartz, M. C.; Barlow, J. W.; Paul, D. R. J Appl Polym Sci 1988, 35, 2053.
2. Machado, J. M.; Lee, C. S. Polym Eng Sci 1994, 34, 59.
3. Halavata, D.; Horak, Z.; Lednicky, F.; Hromadkova, J.; Pleska, A.; Zanevski, Y. V. J Polym Sci Part B: Polym Phys 2001, 39, 931.
4. Dewangan, B.; Jagtap, R. N. Polym Eng Sci 2006, 46, 1147.
5. Faikirov, S. Handbook of Thermoplastic Polyesters; Wiley-vch: Weinheim, 2002.
6. Paul, S.; Kale, D. D. J Appl Polym Sci 2001, 80, 2593.
7. Sinha Ray, S.; Pouliot, S.; Bousmina, M.; Ultracki, L. A. Polymer 2004, 45, 8403.
8. Sinha Ray, S.; Bousmina, M.; Maazouz, A. Polym Eng Sci 2006, 46, 1121.
9. Chen, G. X.; Yoon, J. J Polym Sci Part B: Polym Phys 2005, 43, 478.
10. Paci, M.; La Mantia, F. P. Polym Degrad Stab 1998, 61, 417.
11. Samperi, F.; Puglisi, C.; Montaudo, G. Polym Degrad Stab 2004, 83, 3.
12. Silva Spinacé, M. A.; De Paoli, M. A. J Appl Polym Sci 2004, 91, 525.

13. Escala, A.; Stein, R. S. Adv Chem Ser 1979, 176, 455.
14. Saheb, N.; Jog, D. J. Polym Sci Part B: Polym Phys 1999, 37, 2439.
15. Swoboda, B.; Buonomo, S.; Leroy, E.; Lopez Cuesta, J. M. Polym Degrad Stab 2007, 92, 2247.
16. Swoboda, B.; Buonomo, S.; Leroy, E.; Lopez Cuesta, J. M. Polym Degrad Stab 2008, 93, 910.
17. Huang, J. M.; Chang, F. C. J Appl Polym Sci 2002, 84, 850.
18. Pracella, M.; Rolla, L.; Chionna, D.; Galeski, A. Macromol Chem Phys 2002, 10, 203.
19. Subramanian, P. M.; Mehra, V. Polym Eng Sci 1987, 27, 663.
20. Wood, A. S. Mod Plast 1979, 56, 44.
21. Nadkarni, V. M.; Jog, J. P. Polym Eng Sci 2004, 27, 451.
22. Al-Mulla, A. Express Polym Lett 2007, 01, 334.
23. Bishara, A.; Shaban, H. I. J Appl Polym Sci 2006, 101, 3565.
24. Mallette, J. G.; Marquez, A. Polym Eng Sci 2000, 40, 2272.
25. Messersmith, P. B.; Stupp, S. I. J Mater Res 1992, 7, 2559.
26. Khanna, Y. P. Polym Eng Sci 1990, 30, 1615.
27. Sinha Ray, S.; Okamoto, M. Prog Polym Sci 2003, 28, 1539.
28. Wang, Y.; Gao, J.; Ma, Y.; Agarwal, U. S. Compos B 2006, 37, 399.
29. Liu, Z.; Chen, K.; Yan, D. J Polym Test 2004, 23, 323.